Stiffness, strain and blood volume, unraveling three (mechanical) properties of the brain

Andrej Shoykhet

Abstract—**Mechanical properties of the brain can be indicators for different kinds of brain diseases. Separate measurements of different mechanical properties exist, however, little is known about their mutual influence. This study aims to unravel the influences of shear stiffness, volumetric strain, octahedral shear strain and cerebral blood volume (CBV) in the human brain. Repeated acquisitions of the intrinsic brain movement of 8 healthy subjects using a Displacement ENcoding with Stimulated Echos (DENSE) sequence in a 7T MRI were undertaken to calculate shear stiffness, volumetric strain and octahedral shear strain. Shear stiffness was estimated using intrinsic Magnetic Resonance Elastography (MRE) with nonlinear inversion. Volumetric stain and octahedral shear strain were calculated directly form displacement measurements. CBV values were taken from a brain atlas. We calculated and compared average stiffness, strain and CBV values in 30 regions of interest located in the cortical gray matter (GM), subcortical GM and white matter (WM). The results show a correlation between CBV and strain values in WM regions as well as correlations between volumetric strain and octahedral shear strain. We did not find significant correlations between stiffness and strain. We assume that shear stiffness carries independent information from strain and could thus potentially be indicators for different types of disorders or diseases.**

Index Terms—**MR brain Elastography, volumetric strain, octahedral shear strain, shear stiffness, cerebral blood volume.**

I. INTRODUCTION

THE human brain is a very vulnerable organ and highly sensible to mechanical impact. Therefore, it is the only organ which is almost entirely surrounded by bones and suspended in a liquid for protection against mechanical influence. For some fields of brain research and diagnostics, mechanical properties of the brain, such as shear stiffness, volumetric strain or octahedral shear strain are of interest. Altered brain stiffness could be an indicator for Alzheimer [1], [2] or tumors [3]. Whereas palpation, as it is done for muscles or inner organs is not an option for the brain, it is possible to measure brain stiffness using Magnetic Resonance Elastography (MRE). MRE relies on measuring tissue deformation and fitting a mechanical model that could explain such deformation. During a classical MRE, an external actuator induces shear waves into the tissue. With phase contrast Magnetic Resonance (MR) the propagation of these shear waves is measured in the tissue. Knowing the shear wave propagation, it is possible to solve the underlying differential equations and calculate the shear stiffness. It is, however, possible to perform brain MRE without an extrinsic actuator. This so-called intrinsic MRE exploits the heartbeat-induced movement

Supervisor: Jacobus Zwanenburg
Daily Supervisor: Marius Burman Ingeberg

of the brain. With each heartbeat brain tissue moves in a slight, but repetitive way. From this intrinsic brain movement strain and stiffness can be calculated or estimated, respectively [4], [5], [6], [7], [8]. Removing the external actuator simplifies the measurement setup, overcomes the problem of poor shear wave penetration through the skull and measures the brain in its natural state rather than an artificial vibration state which stiffens the brain [8], [9].

It is suggested that brain tissue stiffens with an increased perfusion of the brain [10]. Strain in the brain is caused by inflow and outflow of blood in the microvasculature in brain tissue. Volumetric strain in gray matter (GM) is higher than in white matter (WM) [5]. However the causes for this difference are unknown. Thanks to our shear stiffness estimation with intrinsic MRE we were able to obtain volumetric strain, octahedral shear strain and shear stiffness values from the same acquisitions. This allowed us to investigate their influence on each other. Using an existing cerebral blood volume (CBV) atlas we additionally investigated the influence of CBV on mechanical brain properties.

This study aims to unravel the potentially mutual influence between volumetric strain, octahedral shear strain, shear stiffness and CBV in the brain.

II. MATERIALS AND METHODS

A. Used data

In this study shear stiffness was compared to volumetric strain, octahedral shear strain and blood volume in the brain. While shear stiffness and strain data were calculated from in house acquisitions, a brain atlas was used for CBV data [11].

1) Utilized data: We used Displacement ENcoding with Stimulated Echos (DENSE) acquisitions of 8 healthy subjects (mean age: 27 ± 6, 3 females). The acquisitions were performed as part of a previous work on brain pulsation [5] and were also used in another publication to estimate brain shear stiffness [8]. Here, we only describe the key aspects of the acquisition and the subsequent data preparation. Acquisitions were done twice for each subject with a break of 10 minutes in between acquisitions. Acquisitions were made using a 7T MR scanner (Philips Healthcare) (Resolution for DENSE 1.95 mm x 1.95 mm x 2.2 mm). Measurements were synchronized with the cardiac cycle and reconstructed with 20 time points per cardiac cycle. For each DENSE cine acquisition a T1-weighted anatomical scan was taken (resolution 0.93 mm x 0.93 mm x 1.00 mm) for image registration and segmentation. Brain tissue probability maps (for GM, WM, Cerebrospinal fluid (CSF)) were generated using Statistical Parametric Mapping software (SPM12 v7487, University College London, London, UK).

A more detailed explanation of the acquisition and data preparation can be found in the original publication [5].

a) Volumetric strain and octahedral shear strain: The volumetric strain ε_v and octahedral shear strain ε_{oss} were calculated directly from the displacement data. Therefore first the strain tensor $\vec{\varepsilon}$ was calculated (eq. (1) with u, v and w being the displacements in x, y and z directions).

$$\begin{aligned}\vec{\varepsilon} &= \begin{pmatrix} \varepsilon_{xx} & \varepsilon_{xy} & \varepsilon_{xz} \\ \varepsilon_{yx} & \varepsilon_{yy} & \varepsilon_{yz} \\ \varepsilon_{zx} & \varepsilon_{zy} & \varepsilon_{zz} \end{pmatrix} \\ &= \begin{pmatrix} \frac{du}{dx} & \frac{1}{2}(\frac{du}{dy}+\frac{dv}{dx}) & \frac{1}{2}(\frac{du}{dz}+\frac{dw}{dx}) \\ \frac{1}{2}(\frac{dv}{dx}+\frac{du}{dy}) & \frac{dv}{dy} & \frac{1}{2}(\frac{dv}{dz}+\frac{dw}{dy}) \\ \frac{1}{2}(\frac{du}{dz}+\frac{dw}{dx}) & \frac{1}{2}(\frac{dw}{dy}+\frac{dv}{dz}) & \frac{dw}{dz} \end{pmatrix}\end{aligned} \quad (1)$$

Volumetric strain is the measurement of voxel-wise expansion and contraction of the tissue [4]. It can be calculated by taking the trace of the strain tensor (eq. (2)).

$$\varepsilon_v = \varepsilon_{xx} + \varepsilon_{yy} + \varepsilon_{zz} \quad (2)$$

Octahedral shear strain is a measurement of the anisotropic deformation of tissue in a voxel. If tissue expands or contracts in all directions by a similar rate then octahedral shear strain is zero. The higher the difference of expansion or contraction in different direction is, the higher is octahedral shear strain. octahedral shear strain can be calculated as in eq. (3) [12].

$$\varepsilon_{oss} = \frac{2}{3}\sqrt{\begin{array}{l}(\varepsilon_{xx}-\varepsilon_{yy})^2+(\varepsilon_{xx}-\varepsilon_{zz})^2+(\varepsilon_{yy}-\varepsilon_{zz})^2 \\ +6(\varepsilon_{xy}^2+\varepsilon_{xz}^2+\varepsilon_{yz}^2)\end{array}} \quad (3)$$

Voxels with very high strain values were considered as artifacts. When during at least half of the heartcycle volumetric strain or octahedral shear strain voxels were higher than 1% or 3% , respectively, they were removed. To minimize partial volume effects for the later analysis tissue probability masks were used to remove all voxels that had a lower probability than 0.95 for both GM and WM were removed.
Throughout the following of this paper we occasionally use simply strain when referring to both volumetric stain and octahedral shear strain at the same time.

b) Shear stiffness: Shear stiffness maps for the used acquisition were available from a previous study [8]. Also here we describe only the key elements of the data generation. An iterative non-linear inversion was performed to minimize the difference between the actually measured displacement and a computational finite element model (FEM) (isotropic mesh size 2.0 mm). In the estimations the lambda modulus was assumed to be constant over the whole brain. Due to the nature of the inversion problem the estimated complex shear modulus G is a relative value. In this study we only used the shear stiffness μ wich can be calculated from the shear modulus by $\mu = \frac{2|G|^2}{Re(G)+|G|}$.
A detailed explanation of the shear stiffness estimation can be found in the original publication [8].

2) CBV: The influence of CBV on strain and shear stiffness was investigated using a CBV atlas in MNI-ICBM2009c space [11]. The atlas originates from 134 MRI scans of patients diagnosed with glioblastoma grade IV, however, voxels affected by the tumor lesion were excluded. The CBV atlas was registered to each patient with Elastix [13]. Therefore the T1 weighted MNI template was registered to each subject and then the same transformations were applied to the CBV atlas. A rigid registration aligning the atlas template to our acquisitions was followed by a affine and b-spline registration to match brain regions.

B. Comparison

A linear regression analysis was performed for the previously described values in a selection of regions of interst (ROIs). Linear regressions were weighted by the size of regions of interst (ROIs).

1) ROIs: Shear stiffness, volumetric strain, octahedral shear strain and CBV were compared using the same 30 brain regions as used for shear stiffness estimations by Hicox et al. [14] and Burman Ingeberg et al. [8]. The regions were based on three brain atlases (MNI-ICBM2009c nonlinear symmetric 1 mm [11], JHU-ICBM-tracts 2 mm and JHU-ICBM-labels 2 mm). The JHU-ICBM atlases were interpolated to match the resolution of the MNI-ICBM2009c template. The registration of the regions atlases was performed in the same way as described above for the CBV atlas. The ROIs were divided into the global ROIs WM, cortical GM and subcortical GM (table II). To ensure that ROIs which were associated with GM only contain GM tissue and ROIs which were associated with WM contain only WM tissue, GM and WM were masked using the tissue probability maps with a threshold of 0.95, before masking by ROI.
In order to compare volumetric strain and octahedral shear strain to shear stiffness and CBV, the time dimension of strain data was reduced by taking only peak to peak volumetric strain and peak octahedral shear strain. The first step was to calculate the average volumetric strain and octahedral shear strain in each region for each timepoint. Then for each region the peak to peak volumetric strain and peak octahedral shear strain were used. Shear stiffness, volumetric strain, octahedral shear strain and CBV were compared pairwise. For each pair, a linear regression was performed once for all brain regions and once separately for WM, cortical GM and subcortical GM.

III. RESULTS

Out of the 8 subjects, 1 was excluded from the analysis due to a high noise level in DENSE acquisitions in the first of the two acquisitions. Figure 1 shows representative maps of volumetric strain (a), octahedral shear strain (b), shear stiffness (c), CBV (d), and an anatomical scan (e). Shear stiffness has a lower spatial variance than volumetric strain or octahedral shear strain.

A. Volumetric strain and octahedral shear strain

The volumetric strain and octahedral shear strain correlated positively between the ROIs. With an R^2 value of 0.448 and a p-value of <0.001 (table I and Supplementary Material) in a linear regression over all brain regions this is the strongest correlation within the analyzed values. In addition, the linear regression showed a significant correlation WM (fig. 2a).

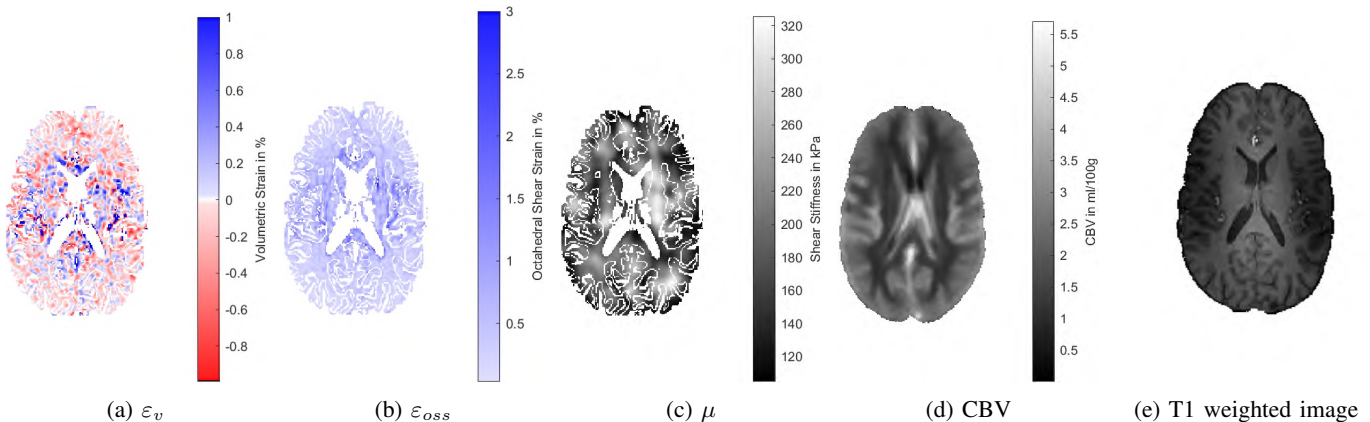(a) ε_v (b) ε_{oss} (c) μ (d) CBV   (e) T1 weighted image

Fig. 1: Representative maps of volumetric strain (a), octahedral shear strain (b), shear stiffness (c), CBV (d) and the T1-weighted image (e) for subject 2 (measurement 1). Strain images are at the moment of peak strain across the brain. Stiffness and strain images are masked preserving only regions where probability maps of GM or WM had a value higher than 0.95.

TABLE I: Results of weighted linear regression using all 30 ROIs. Only ε_v and ε_{oss} show significant correlation.

independent	dependent	R^2	p-Value	slope	intercept
μ	ε_v	< 0.001	0.902	6.4e-07	0.00095
μ	ε_{oss}	< 0.001	0.985	-4.3e-07	0.0070
CBV	μ	0.143	0.040	-13.768	248.0056
CBV	ε_v	0.071	0.154	0.00026	0.00054
CBV	ε_{oss}	0.012	0.572	0.00048	0.0059
ε_{oss}	ε_v	0.449	< 0.001	0.14867	7.1888e-05

B. CBV and strain

For both volumetric strain and octahedral shear strain a significant correlation with CBV was found for WM regions. No significant correlations were found for GM or the whole brain (figs. 2b and 2c and table I and Supplementary Material).

C. Shear stiffness and strain

For all three global brain regions and both volumetric strain and octahedral shear strain the linear regression does not show significant correlations between strain and shear stiffness (figures 2d and 2e). The ROIs are distributed over the strain and shear stiffness values. No big differences between WM, subcortical GM and cortical GM were found. Also a linear regression over all ROIs did not show a significant relationship between shear stiffness and strain (table I and Supplementary Material).

D. CBV and shear stiffness

A significant negative correlation was measured for shear stiffness and CBV over all brain regions (table I and Supplementary Material). There was no significant correlation when comparing CBV and strain in the three global brain regions separately.

IV. DISCUSSION

We used displacement measurements of 8 human brains and extracted shear stiffness, volumetric strain and octahedral shear strain within the brain. Taking the advantage of having strain and shear stiffness values from the same measurements, we compared those two values to understand underlying relationships between these values in the brain. Furthermore, we used a CBV atlas to also investigate the influence of blood volume in the brain on strain and shear stiffness. We analyzed the interaction between these values in a selection of ROIs. We did not find any strong correlations between shear stiffness and volumetric strain or shear stiffness and octahedral shear strain. In WM regions both volumetric stain and octahedral shear strain correlated with CBV. Shear stiffness correlated with CBV when taking into account all ROIs, but not in our subselection of global ROIs. Furthermore volumetric strain correlated with octahedral shear strain when analyzing the whole brain and when analysing WM regions separately. To the best of our knowledge this is the first study that compares brain stiffness and strain.

A. Volumetric and octahedral shear strain

Volumetric strain and octahedral shear strain represent different strain states of tissue. A shape-preserving but volume-changing deformation leads to volumetric strain but not to octahedral shear strain. A isovolumetric deformation that changes the shape leads to octahedral shear strain but not to volumetric strain. In the brain, peak to peak volumetric strain correlates positively with peak octahedral shear strain between the selected ROIs. This shows that high expansion or contraction of brain tissue is often accompanied by deformation of that tissue and is seldom uniform in all directions. However, Sloots et al.[6] claimed that volumetric strain and octahedral shear strain do not correlate significantly. Whereas Sloots et al. compared volumetric strain and octahedral shear strain on a voxel basis, we assessed at peak strain values and averaged over big regions. If neighbouring voxels to voxels with high volumetric strain show a high octahedral shear stain there will be a correlation in our analysis but not in the analysis by Sloots et al. Furthermore, Sloots et al. compared the values for peak systole whereas we took the peak value for each region regardless of the timepoint. Therefore, these two analyses are not comparable exaclty and do not necessarily contradict.
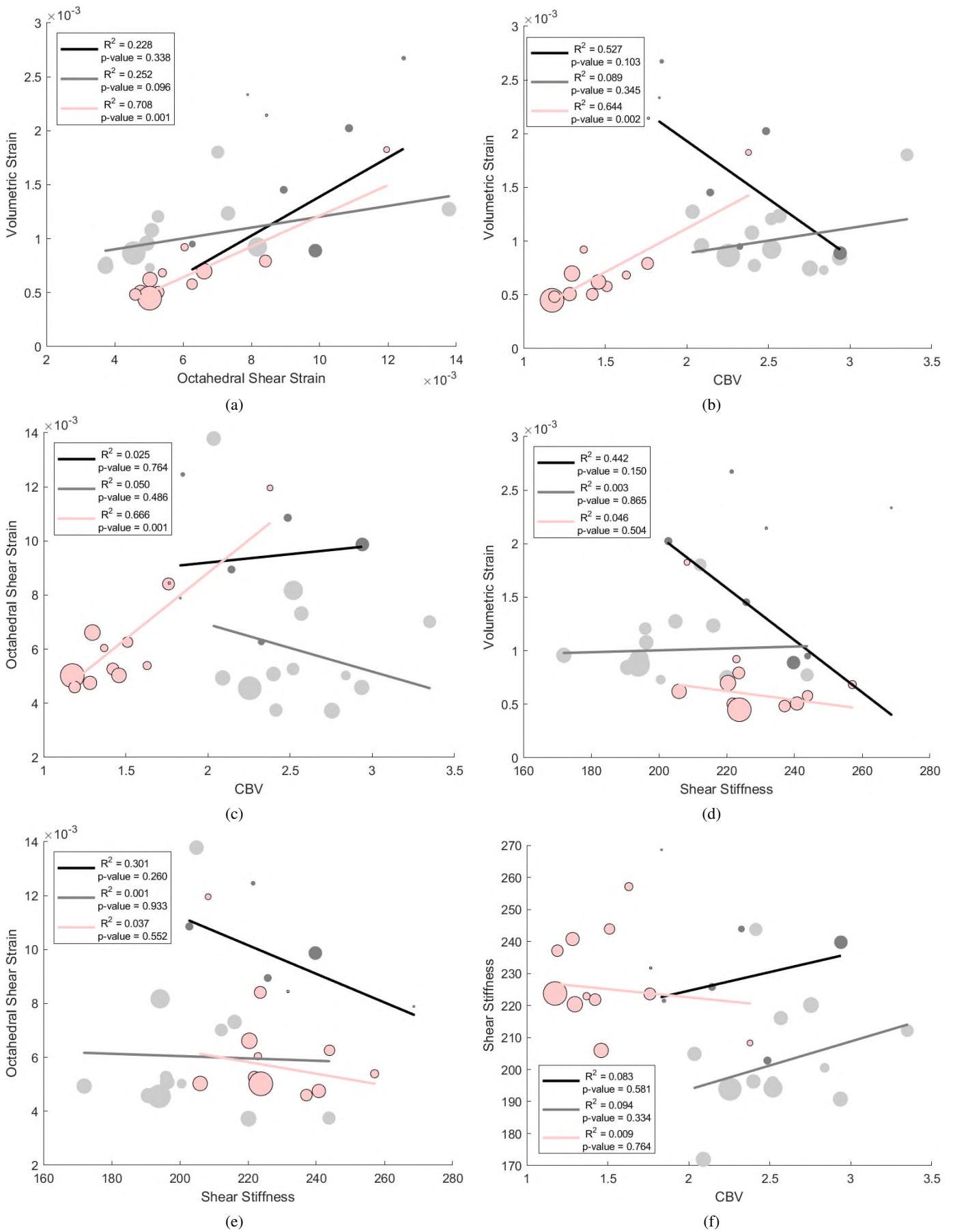
Fig. 2: Results of weighted linear regression for each quantity of interest, separately for three global ROIs. Each circle represents one ROI. The size of the circle indicates the size of the ROI. WM regions are in red, cortical GM regions and subcortical GM regions light gray and dark gray respectively. The exact values are presented in table II

TABLE II: Average values of volumetric strain, octahedral shear strain, shear stiffness, CBV, and size of the ROI for each ROI across all considered measurements. WM regions are highlighted in red, cortical GM regions and subcortical GM regions light gray and dark gray respectively.

Region Name	ε_v in %	ε_{oss} in %	shear stiffness in kPa	CBV in $\frac{g}{100ml}$	Region size in voxel	atlas
Cuneus	0.07	0.5	200.53	2.84	6249	CerebrA
Fusiform Gyrus	0.12	0.73	216.04	2.57	13430	CerebrA
Inferior Temporal Cortex	0.13	1.38	204.88	2.04	13462	CerebrA
Lateral Occipital Cortex	0.08	0.46	190.76	2.94	15007	CerebrA
Lingual Occipital Cortex	0.18	0.7	212.15	3.35	10800	CerebrA
Precuneus	0.07	0.37	220.12	2.75	16248	CerebrA
Postcentral Cortex	0.12	0.53	195.98	2.52	10416	CerebrA
Rostral Middle Frontal Cortex	0.1	0.49	171.95	2.09	15117	CerebrA
Superior Frontal Cortex	0.09	0.46	193.92	2.25	35256	CerebrA
Superior Parietal Cortex	0.08	0.37	243.72	2.41	11348	CerebrA
Superior Temporal Cortex	0.09	0.82	194.21	2.52	23826	CerebrA
Precentral Cortex	0.11	0.51	196.28	2.4	13750	CerebrA
Amygdala	0.27	1.25	221.47	1.85	1350	CerebrA
Caudate	0.15	0.89	225.78	2.14	4049	CerebrA
Hippocampus	0.2	1.09	202.79	2.49	4333	CerebrA
Pallidum	0.23	0.79	268.6	1.83	572	CerebrA
Putamen	0.1	0.63	243.88	2.32	2978	CerebrA
Thalamus	0.09	0.99	239.73	2.94	11946	CerebrA
Anterior Thalamic Radiation	0.06	0.63	243.87	1.51	7051	ICBM Tracts
Corticospinal Tract	0.08	0.84	223.58	1.76	9066	ICBM Tracts
Major Forceps	0.07	0.54	257.1	1.63	4317	ICBM Tracts
Minor Forceps	0.05	0.48	240.75	1.28	11368	ICBM Tracts
Inferior Frontal Occipital Fasciculus	0.05	0.53	221.81	1.42	8935	ICBM Tracts
Inferior Longitudinal Fasciculus	0.09	0.6	222.88	1.37	3534	ICBM Tracts
Superior Longitudinal Fasciculus	0.06	0.5	205.96	1.46	13494	ICBM Tracts
Uncinate Fasciculus	0.21	0.84	231.69	1.76	366	ICBM Tracts
Corpus Callosum	0.07	0.66	220.38	1.3	15441	ICBM Labels
Corona Radiata	0.04	0.5	223.74	1.17	35851	ICBM Labels
Fornix	0.18	1.2	208.29	2.38	2253	ICBM Labels
Posterior Thalamic Radiation	0.05	0.46	237.1	1.19	8627	ICBM Labels

B. Influences on volumetric and octahedral shear strain

Volumetric strain in brain tissue is caused by a change of blood volume in the tissue. Brain tissue expands due to blood inflow in the microvasculature and contracts with blood outflow of the microvasulature. Adams et al. [5] showed that volumetric strain in GM is higher and has an earlier peak than in WM for the same acquisitions as used in this study. There is, however, little evidence on the causes of variations in volumetric strain. (For the following discussion we also assume a uniform blood pressure in the whole brain for every given timepoint). In a hypothetical brain, where tissue stiffness, vessel wall stiffness and vessel radii are uniform across the whole brain and only the CBV is different across brain regions, CBV would be the driving factor for volumetric strain. A higher blood volume yields a higher volumetric strain for the same relative blood volume change. In our analysis volumetric strain in WM showed significant correlation with CBV. In line with our observations in WM is an influence of CBV on volumetric strain. Another possible factor for volumetric strain variations could be tissue stiffness. However, we did not find significant positive or negative correlation between volumetric strain and shear stiffness. One could also assume that a higher shear stiffness would lead to lower volumetric strain within the tissue. However, it might be more fitting to compare the lambda modulus (compression modulus) to volumetric strain, however we did have estimations of the lambda modulus across the brain.

Other factors which were not analyzed in this study but which could also influence volumetric strain could be vessel wall stiffness and vessel radii. Vessel wall stiffness in microvasculatrue is an unknown factor but could be predominant for the amplitude of volumetric strain. If variations in vessel wall stiffness are higher than in brain tissue stiffness and if vessel walls are stiffer than the surrounding tissue, then brain tissue stiffness is negligible for volumetric strain. Vessel radii are different within the brain and can change for example during hypercapnia [15]. For the a given CBV different vessel radii lead to different vessel wall surface. For small vessel radii there have to be more vessels for a given CBV, which results in a higher vessel surface than less vessels with a bigger radii. During a pressure change (due to the pulse) a bigger surface leads to a higher applied force which leads to higher volumetric strain. We conclude that volumetric strain is not strongly influenced by shear stiffness and further analysis has to be done to understand reasons for variations of volumetric strain.

We have also found that also octahedral shear strain correlated with CBV. After seeing a positive correlation between volumetric strain and octahedral shear strain, as well as volumetric strain and CBV the correlation between octahedral shear strain and CBV can be expected.

We did not find significant positive or negative correlation between octahedral shear strain and shear stiffness. An explanation for the lack of correlation between octahedral shear strain and shear stiffness might be the effect boundary conditions and the complex shape of the brain. Ventricles, suculi, fissures

and boundaries between the subdivisions of the brain create tissue boundaries within the brain. It is possible that separate structures in the brain can move somewhat independently to each other. In that case not low shear stiffness, but the shape causes high strain regions. This hypothesis could be proved by a modelling different deformations of the human brain considering it's shape and analyzing regions where high strains occur. A more local analysis of might also give insight in the influence of shape on octahedral shear strain but is difficult due to high noise levels.

C. Shear stiffness and CBV

We observed a significant negative correlation between brain shear stiffness and CBV over the whole brain. However with an R^2 of 0.142 there is a high of variance in this correlation. We assume that the correlation appears due to a in general higher shear stiffness in of WM than in GM and a lower CBV in WM than in GM. Within the global ROIs (WM, cortical GM and subcortical GM) no correlation between CBV and shear stiffness was found.

Multiple studies report influence of brain perfusion on the brain stiffness. Hetzer et al. reported that with a higher perfusion deep GM has a higher magnitude of the shear modulus G [16]. (Deep GM almost corresponds to what is called subcortical GM in this study except that the Caudate is not part of deep GM [16] and the Nucleus accumbens is not part of subcortical GM in this study). In a subsequent study, Hetzer et al. showed that hypercapnia influences the shear modulus [10]. It is known that hypercapnia leads to a widening of the microvasculature in the brain and thereby increases perfusion [15]. Hetzer et al. explain a increase of the shear modulus magnitude partially with a variable viscosity of blood. The Lahraeus-Lindqvist effect [17] states, that blood viscosity increases in smaller vessels. An increased perfusion of the same brain region means a increased vascular crossection leading to a decreased blood viscosity. This change in blood viscosity also changes the shear modulus in the brain. Also in ultrasound elastography measurements an increase in shear wave speed (which correlates positively with the shear modulus) was reported [18].

Performing the valsalva manoever also increases temporarily brain shear stiffness in MRE measurements [19], as well as an increase in shear wave speed in ultrasound elastography measurements [20]. One known condition that decreases shear stiffness is high intensity exercise [21]. Directly after high intensity exercise, the shear stiffness is significantly lower than before or one hour after the exercise. The magnitude of the shear stiffness changes are dependent on the brain region.

In the mentioned studies brain the shear modulus, shear wave speed and shear stiffness change with a change of cerebral blood flow (CBF). Further research needs to be performed in order to conclude, whether brain shear stiffness is coupled to CBF without being strongly influenced by CBV.

D. Limitations

We took advantage of having strain and shear stiffness values from the same measurements and did not find any correlation between strain and shear stiffness. However, for CBV values we had to rely on a brain atlas. This can cause registration errors, where corresponding voxels are not perfectly aligned, and does not take into account physiological differences between subjects. Also the use of atlases for the regional comparison yields some registration errors. However, an initially tried voxel-wise comparison showed so much noise, that no correlations could be detected. By averaging strain values over ROIs, we minimized the effect of outliers and noise.

More powerful statistical methods such as multilevel statistical analysis could be tried to find more subtle relationships between the analyzed values. For the certainty of our results we decided to use a linear regression analysis.

E. Outlook

We discussed different aspects on the influence of shear stiffness on strain, of CBV on stiffness and of CBV on strain. While in our study we regarded shear stiffness as a given tissue property, it was shown other studies that shear stiffness itself is subject of change depending on brain perfusion [10], [16], [18], [20] and can change after physical exercise [21]. For a thorough understanding of mechanical brain tissue properties, multiple parameters should be assessed simultaneously. Furthermore, some factors, such as blood pressure or CSF pressure were not taken into account though they might influence results.

V. CONCLUSION

In this study we analyzed mechanical properties of the brain. Volumetric strain, octahedral shear strain and shear stiffness were calculated from 7T MR displacement measurements of intrinsic brain movement. Cerebral blood volume values were taken from a MNI brain atlas. Correlations between CBV and strain in WM regions were found as well as between volumetric and octahedral shear strain. Mechanical strain was found to be not influenced by brain shear stiffness. We assume some detected correlations between CBV and shear stiffness may lack due to a high variance. We conclude that the analyzed stain and stiffness data reflects different underlying properties of the brain and might be indicators for different kinds of disorders.

VI. LAYMEN'S SUMMARY

By putting fingers on the correct location of the wrist it is possible to feel the pulse. If one could look through the skin, it would also be possible to see the pulsating blood vessel. With special Magnetic resonance examinations such a pulsation can be measured in the brain. This is very interesting and useful, since we cannot simply look into or touch the brain. The pulsating blood makes the brain move a little bit with each heartbeat. By measuring these movements it is possible to see where the brain gets stretched but also to find parts of the brain which are softer or stiffer than other parts. Knowing stiff and soft regions of the brain can help to find out more about diseases such as Alzheimer's or cancer. But before being able to link brain movement and stiffness to diseases we have

to understand movement and stiffness in the healthy brain. We analyzed how brain motion and stiffness relate to each other and if the amount of blood in the brain changes brain motion or stiffness. This research should help to better understand diseases and in the future help to diagnose some diseases earlier, so that they can be treated better.

REFERENCES

[1] M. ElSheikh, A. Arani, A. Perry, B. F. Boeve, F. B. Meyer, R. Savica, R. L. Ehman, and J. Huston, "MR Elastography Demonstrates Unique Regional Brain Stiffness Patterns in Dementias," *American Journal of Roentgenology*, vol. 209, no. 2, pp. 403–408, Aug. 2017, publisher: American Roentgen Ray Society. [Online]. Available: https://www.ajronline.org/doi/10.2214/AJR.16.17455

[2] M. C. Murphy, J. Huston III, C. R. Jack Jr, K. J. Glaser, A. Manduca, J. P. Felmlee, and R. L. Ehman, "Decreased brain stiffness in Alzheimer's disease determined by magnetic resonance elastography," *Journal of Magnetic Resonance Imaging*, vol. 34, no. 3, pp. 494–498, 2011, _eprint: https://onlinelibrary.wiley.com/doi/pdf/10.1002/jmri.22707. [Online]. Available: https://onlinelibrary.wiley.com/doi/abs/10.1002/jmri.22707

[3] A. Bunevicius, K. Schregel, R. Sinkus, A. Golby, and S. Patz, "REVIEW: MR elastography of brain tumors," *NeuroImage: Clinical*, vol. 25, p. 102109, Jan. 2020. [Online]. Available: https://www.sciencedirect.com/science/article/pii/S2213158219304565

[4] A. L. Adams, H. J. Kuijf, M. A. Viergever, P. R. Luijten, and J. J. Zwanenburg, "Quantifying cardiac-induced brain tissue expansion using DENSE," *NMR in Biomedicine*, vol. 32, no. 2, p. e4050, 2019, _eprint: https://onlinelibrary.wiley.com/doi/pdf/10.1002/nbm.4050. [Online]. Available: https://onlinelibrary.wiley.com/doi/abs/10.1002/nbm.4050

[5] A. L. Adams, M. A. Viergever, P. R. Luijten, and J. J. M. Zwanenburg, "Validating faster DENSE measurements of cardiac-induced brain tissue expansion as a potential tool for investigating cerebral microvascular pulsations," *NeuroImage*, vol. 208, p. 116466, Mar. 2020. [Online]. Available: https://www.sciencedirect.com/science/article/pii/S1053811919310572

[6] J. J. Sloots, G. J. Biessels, A. de Luca, and J. J. M. Zwanenburg, "Strain Tensor Imaging: Cardiac-induced brain tissue deformation in humans quantified with high-field MRI," *NeuroImage*, vol. 236, p. 118078, Aug. 2021. [Online]. Available: https://www.sciencedirect.com/science/article/pii/S1053811921003554

[7] S. Hirsch, D. Klatt, F. Freimann, M. Scheel, J. Braun, and I. Sack, "In vivo measurement of volumetric strain in the human brain induced by arterial pulsation and harmonic waves," *Magnetic Resonance in Medicine*, vol. 70, no. 3, pp. 671–683, 2013, _eprint: https://onlinelibrary.wiley.com/doi/pdf/10.1002/mrm.24499. [Online]. Available: https://onlinelibrary.wiley.com/doi/abs/10.1002/mrm.24499

[8] M. Burman Ingeberg, E. Van Houten, and J. J. M. Zwanenburg, "Estimating the viscoelastic properties of the human brain at 7 T MRI using intrinsic MRE and nonlinear inversion," *Human Brain Mapping*, vol. 44, no. 18, pp. 6575–6591, 2023, _eprint: https://onlinelibrary.wiley.com/doi/pdf/10.1002/hbm.26524. [Online]. Available: https://onlinelibrary.wiley.com/doi/abs/10.1002/hbm.26524

[9] H. Herthum, S. C. H. Dempsey, A. Samani, F. Schrank, M. Shahryari, C. Warmuth, H. Tzschätzsch, J. Braun, and I. Sack, "Superviscous properties of the in vivo brain at large scales," *Acta Biomaterialia*, vol. 121, pp. 393–404, Feb. 2021.

[10] S. Hetzer, F. Dittmann, K. Bormann, S. Hirsch, A. Lipp, D. J. Wang, J. Braun, and I. Sack, "Hypercapnia increases brain viscoelasticity," *Journal of Cerebral Blood Flow & Metabolism*, vol. 39, no. 12, pp. 2445–2455, Dec. 2019. [Online]. Available: https://www.ncbi.nlm.nih.gov/pmc/articles/PMC6893988/

[11] E. Fuster-Garcia, J. Juan Albarracín, I. T. Hovden, M. d. M. Álvarez Torres, A. Rovira, L. Oleaga, A. J. Revert, S. Filice, J. M. García-Gómez, and K. E. Emblem, "eliesfuster/cbv_atlas: CBV BRAIN ATLAS v1," May 2021. [Online]. Available: https://zenodo.org/records/4757126

[12] M. D. J. McGarry, E. E. W. V. Houten, P. R. Perriñez, A. J. Pattison, J. B. Weaver, and K. D. Paulsen, "An octahedral shear strain-based measure of SNR for 3D MR elastography," *Physics in Medicine & Biology*, vol. 56, no. 13, p. N153, Jun. 2011. [Online]. Available: https://dx.doi.org/10.1088/0031-9155/56/13/N02

[13] S. Klein, M. Staring, K. Murphy, M. A. Viergever, and J. P. W. Pluim, "elastix: A Toolbox for Intensity-Based Medical Image Registration," *IEEE Transactions on Medical Imaging*, vol. 29, no. 1, pp. 196–205, Jan. 2010, conference Name: IEEE Transactions on Medical Imaging. [Online]. Available: https://ieeexplore.ieee.org/document/5338015

[14] L. V. Hiscox, M. D. J. McGarry, H. Schwarb, E. E. W. Van Houten, R. T. Pohlig, N. Roberts, G. R. Huesmann, A. Z. Burzynska, B. P. Sutton, C. H. Hillman, A. F. Kramer, N. J. Cohen, A. K. Barbey, K. D. Paulsen, and C. L. Johnson, "Standard-space atlas of the viscoelastic properties of the human brain," *Human Brain Mapping*, vol. 41, no. 18, pp. 5282–5300, 2020, _eprint: https://onlinelibrary.wiley.com/doi/pdf/10.1002/hbm.25192. [Online]. Available: https://onlinelibrary.wiley.com/doi/abs/10.1002/hbm.25192

[15] Y. Shen, I. M. Pu, T. Ahearn, M. Clemence, and C. Schwarzbauer, "Quantification of venous vessel size in human brain in response to hypercapnia and hyperoxia using magnetic resonance imaging," *Magnetic Resonance in Medicine*, vol. 69, no. 6, pp. 1541–1552, 2013, _eprint: https://onlinelibrary.wiley.com/doi/pdf/10.1002/mrm.24258. [Online]. Available: https://onlinelibrary.wiley.com/doi/abs/10.1002/mrm.24258

[16] S. Hetzer, P. Birr, A. Fehlner, S. Hirsch, F. Dittmann, E. Barnhill, J. Braun, and I. Sack, "Perfusion alters stiffness of deep gray matter," *Journal of Cerebral Blood Flow & Metabolism*, vol. 38, no. 1, pp. 116–125, Jan. 2018, publisher: SAGE Publications Ltd STM. [Online]. Available: https://doi.org/10.1177/0271678X17691530

[17] R. Fåhræus and T. Lindqvist, "The viscosity of the blood in narrow capillary tubes," *American Journal of Physiology-Legacy Content*, vol. 96, no. 3, pp. 562–568, Mar. 1931, publisher: American Physiological Society. [Online]. Available: https://journals.physiology.org/doi/abs/10.1152/ajplegacy.1931.96.3.562

[18] B. Kreft, H. Tzschätzsch, F. Schrank, J. Bergs, K.-J. Streitberger, S. Wäldchen, S. Hetzer, J. Braun, and I. Sack, "Time-Resolved Response of Cerebral Stiffness to Hypercapnia in Humans," *Ultrasound in Medicine & Biology*, vol. 46, no. 4, pp. 936–943, Apr. 2020. [Online]. Available: https://www.sciencedirect.com/science/article/pii/S0301562919316394

[19] H. Herthum, M. Shahryari, H. Tzschätzsch, F. Schrank, C. Warmuth, S. Görner, S. Hetzer, H. Neubauer, J. Pfeuffer, J. Braun, and I. Sack, "Real-Time Multifrequency MR Elastography of the Human Brain Reveals Rapid Changes in Viscoelasticity in Response to the Valsalva Maneuver," *Frontiers in Bioengineering and Biotechnology*, vol. 9, May 2021, publisher: Frontiers. [Online]. Available: https://www.frontiersin.org/journals/bioengineering-and-biotechnology/articles/10.3389/fbioe.2021.666456/full

[20] H. Tzschätzsch, B. Kreft, F. Schrank, J. Bergs, J. Braun, and I. Sack, "In vivo time-harmonic ultrasound elastography of the human brain detects acute cerebral stiffness changes induced by intracranial pressure variations," *Scientific Reports*, vol. 8, no. 1, p. 17888, Dec. 2018, publisher: Nature Publishing Group. [Online]. Available: https://www.nature.com/articles/s41598-018-36191-9

[21] G. McIlvain, E. M. Magoon, R. G. Clements, A. Merritt, L. V. Hiscox, H. Schwarb, and C. L. Johnson, "Acute effects of high-intensity exercise on brain mechanical properties and cognitive function," *Brain Imaging and Behavior*, Mar. 2024. [Online]. Available: https://doi.org/10.1007/s11682-024-00873-y

Supplementary Material:

Results of weighted linear regression for each quantity of interest and all regions within the brain. Each circle represents one ROI. The size of the circle indicates the size of the ROI. WM regions are in red, cortical GM regions and subcortical GM regions light gray and dark gray respectively. The exact values are presented in table II